

Figure 2 The frequency fluctuations of the Zeeman transition under open-loop and closed-loop conditions.

as the C field to be under closed-loop control. The NIST-7 digital servo uses a hydrogen maser as a reference frequency. A low phase-noise synthesizer developed at NIST⁴ is used to generate the microwave interrogation frequency. A slow square-wave modulation technique is used to probe the central Ramsey peak and determine line-center. The difference between the line-center frequency and the maser frequency is logged by a computer for subsequent analysis. Care has been taken to reduce frequency pulling introduced by spurious components of the microwave spectrum that are coherent with the slow square-wave modulation. NIST-7 employs a longitudinal C-field. Consequently, there is a slight sensitivity to changes in the ambient magnetic field due to the reduced effectiveness of the magnetic shields in the longitudinal direction. Figure 2 shows the variation of the Zeeman frequency (and the resulting fractional frequency change of the clock transition) due to changes in the ambient magnetic field. For times less than about 80 000 seconds, the figure shows typical changes in the Zeeman frequency due to a diurnal variation in the local east-west component of the terrestrial magnetic field. This variation is due to an interaction of the solar wind with the Earth's ionosphere. These data show that this diurnal fluctuation in the ambient magnetic field can give rise to a fractional frequency change of a couple parts in 10^{14} . This is twice the uncertainty goal for NIST-7. These frequency fluctuations have been reduced

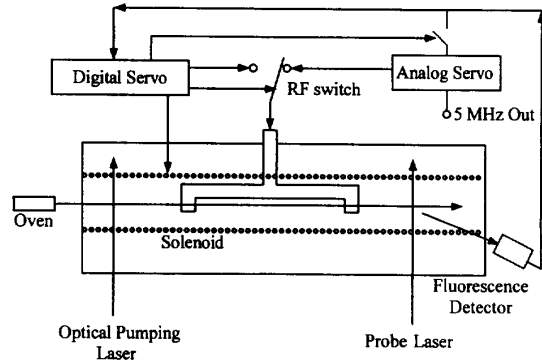


Figure 3 Block diagram of the hybrid servo system.

using a C-field servo, which was implemented using the computer-controlled digital synthesizer. The frequency agility of the digital servo allows monitoring of a field-sensitive transition. The computer uses these data to provide closed-loop control of the C field by adjusting the current in the C field solenoid. Figure 2 shows the performance of the C-field servo for times greater than about 90 000 seconds. Fractional frequency changes in the clock transition due to fluctuations in the ambient magnetic field have been reduced to a few parts in 10^{15} .

Hybrid Servo

The analog servo has a higher modulation rate and, thus, is less sensitive to $1/f$ noise present in the system than the slow digital servo. The digital servo has the ability to provide closed-loop control of the C-field, which is not possible for the present analog servo system. Therefore, a hybrid servo system has been developed. Figure 3 shows the hybrid servo block diagram. A switch controls the RF input to the Ramsey cavity, selecting either the analog or the digital servo. The output power level of these two sources has been closely matched. First, the analog servo interrogates the central Ramsey peak and steers a 5 MHz oscillator to its center. Next, the digital servo interrogates the Zeeman frequency and controls the C field. Finally, the analog servo regains control and continues to probe the Ramsey peak. The 5 MHz oscillator is free running during the digital interrogation interval; therefore, the digital servo should perform its operation in a time that is small compared to the interrogation interval of the analog servo. The time required by the digital servo is less than one second, which does not significantly degrade the stability

of the quartz oscillator. Both the analog and digital portions of the hybrid servo monitor the atomic beam fluorescence. The digital servo does not digitize this signal while the analog servo is operating. However, the analog servo must be electronically disconnected from the beam tube while the digital servo is running. This is necessary because the fluorescence generated by the slow square-wave frequency modulation of the digital servo can degrade the open-loop stability of the analog servo. Similarly, switching transients occurring during the removal of the fluorescence signal can degrade open-loop stability. This is a result of the design of the dual-integrator, frequency-control loop. A switching transient can generate a non-zero error (briefly) which drives the output of the first integrator to some non-zero, constant voltage. Since the analog servo is open loop, the output of the second integrator will grow linearly with time, introducing a linear frequency drift. The upper trace of figure 4 shows the frequency drift of the analog servo under open-loop conditions when the fluorescence signal is disconnected at some arbitrary point in its modulation cycle. The slope of the linear frequency drift can be reduced dramatically if the fluorescence switch timing is phase-locked to the 49 Hz phase modulation clock of the analog servo. Figure 5 shows the timing diagram of the improved system. The time delay, ΔT , from the falling edge of a synchronization marker

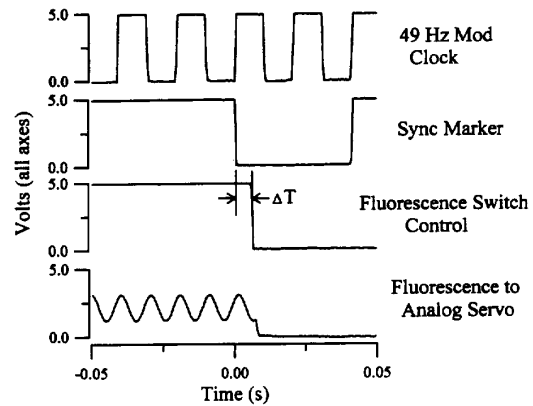


Figure 5 The timing diagram for the hybrid servo switch controls.

to the activation of the fluorescence switch can be adjusted with a resolution of 100 microseconds. This permits fine adjustment of the switching transients and the virtual elimination of the frequency drift of the analog servo while open-loop. The lower trace of figure 4 shows that the residual frequency fluctuations of the analog servo have been reduced to nearly the noise floor of the measurement system. Furthermore, figure 6 indicates that the implementation of the hybrid servo has not significantly degraded the short-term frequency stability of the analog servo.

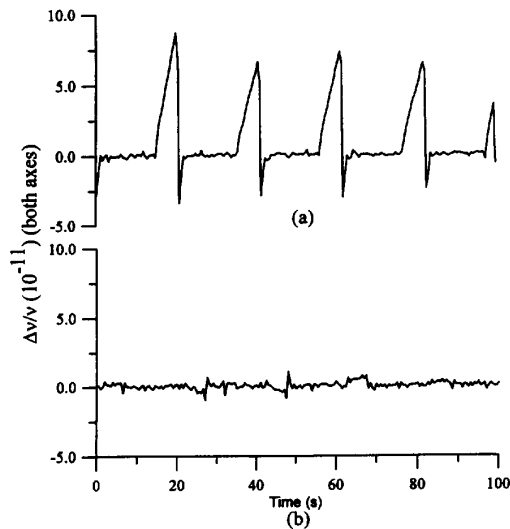


Figure 4 The fractional frequency deviations due to
a) asynchronous and
b) synchronous switching.

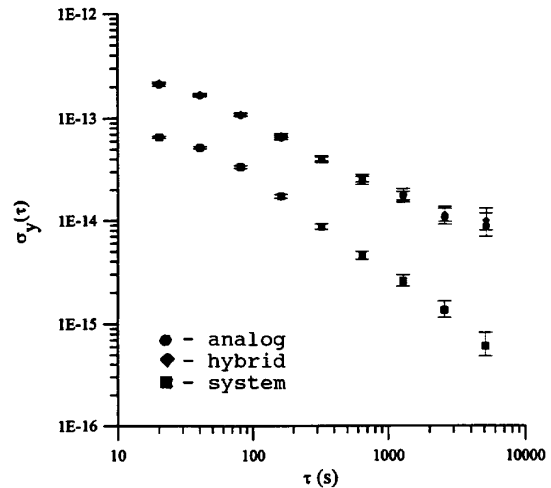


Figure 6 The stability diagram for the hybrid servo.

Conclusion

Using a digital frequency control servo, we have found that active control of the C field is necessary in order to achieve the frequency uncertainty goal for NIST-7. A hybrid digital/analog servo has been designed and implemented. This servo suppresses frequency fluctuations due to the second order Zeeman effect to a few parts in 10^{15} without significantly degrading short-term stability. This hybrid servo also interrogates the central Ramsey peak at a high modulation rate, thus avoiding potential $1/f$ noise. The addition of the digital servo to the existing analog servo system has reduced the uncertainty and has helped facilitate the systematic error analysis.

References

- [1] R.E. Drullinger, J.H. Shirley, J.P. Lowe, and D.J. Glaze, "Error Analysis of the NIST Optically Pumped Primary Frequency Standard", IEEE Transactions on Instrumentation and Measurements, vol. 42, no. 2, pp. 453-456, April 1993
- [2] J.P. Lowe, and F.L. Walls, "Ultralinear Small-angle Phase Modulator", Proceedings of the 5th European Frequency and Time Forum, pp. 461-464, 1991
- [3] L.S. Cutler, and R.P. Giffard, "Architecture and Algorithms for New Cesium Beam Frequency Standard Electronics", Proceedings of the IEEE Frequency Control Symposium, pp. 127-133, 1992
- [4] C.W. Nelson, F.L. Walls, F.G. Ascarunz, and P.A. Pond, "Progress on Prototype Synthesizer Electronics for (199)Hg", Proceedings of IEEE Frequency Control Symposium, pp.64-69, 1992